A spherical element subdivision method for the numerical evaluation of nearly singular integrals in 3D BEM

Jianming Zhang*, Pan Wang, Chenjun Lu, Yunqiao Dong

State Key Laboratory of Advanced Design and Manufacturing for Vehicle Body, College of Mechanical and Vehicle Engineering, Hunan University, Changsha 410082, China

Correspondence to: Jianming Zhang
College of Mechanical and Vehicle Engineering, Hunan University, Changsha 410082, China
Telephone: +86-731-88823061
E-mail: zhangjm@hnu.edu.cn

Abstract

Purpose – A spherical element subdivision method for the numerical evaluation of nearly singular integrals in three-dimensional (3D) boundary element method (BEM) is presented in this paper.

Design/methodology/approach – In this method, the source point is firstly projected to the tangent plane of the element. Then two cases are considered: the projection point is inside or outside the element. In both cases, the element is subdivided into a number of patches using a sequence of spheres with decreasing radius.

Findings – With the proposed method, the patches obtained are automatically refined as they approach the projection point and each patch of the integration element is "good" in shape and size for standard Gaussian quadrature. Therefore, all kinds of nearly singular boundary integrals on elements of any shape and size with arbitrary source point location related to the element can be evaluated accurately and efficiently.

Originality/value – Numerical examples for planar and slender elements with various relative location of the source point are presented. The results demonstrate that our method has much better accuracy, efficiency and stability than conventional methods.

Key Words: BEM, nearly singular integral, element subdivision, Gaussian quadrature

Article Type: Research paper

1. Introduction

Accurate and efficient evaluation of nearly singular integrals has long been an issue of major concern in BEM [1-6]. The nearly singular integrals arise when the source point is close to but not

on the element of integration. These happen in many BEM analyses for engineering problems, such as the analysis of thin or shell-like structures [7-9], the contact problems [10], the sensitivity problems [11] and the displacement around open crack tips [12]. Theoretically, the nearly singular integrals are actually regular since the value of their integrants is finite. However, they are even more difficult to evaluate using the traditional Gaussian quadrature rules. This is because the value of the integrand for varies dramatically as the source point approaches to the element.

Various methods have been proposed to cope with nearly singular integrals, such as analytical and semi-analytical method [13, 14], exponential transformation [15-18], distance transformation [19-21] and sinh transformation [22-25]. As analytical integrals do not exist for a general curved element, the analytical and semi-analytical methods are mainly used for the constant or linear element. As for the above non-linear transformation method, the numerical results are sensitive to the location of the projection point of the source point.

Element subdivision [26, 27] is one of the most widely used methods for evaluating nearly singular integral. Zhang et al. have developed an adaptive element subdivision method using Quad-tree subdivision [5, 28]. In this method, the quadrilateral element is divided into four equal sub-elements which are also called patches. It is performed in the local coordinate system of the element rather than in the physical coordinate system. Obviously, it may produce patches in "bad" shapes in the case that the element is distorted or the element is irregular in shape. As patches in "good" shape in the parametric space may become "bad" when they are mapped into the physical coordinate system. (The word "good" here means that the area of the patch is as large as possible under the condition that the fundamental solution within the patch can be accurately interpolated by low order polynomials.) Besides, this method is not suitable for triangle elements. So far, a general and accurate method for nearly singular integrals is still unavailable.

In this paper, a spherical element subdivision method for the numerical evaluation of nearly singular integrals in 3D BEM is proposed. In this method, an element is subdivided into a number of patches (sub-element) by cutting it using a sequence of spheres with decreasing radius. The patches obtained are automatically refined as they approach the projection point. As a result, each patch is "good" in shape and size for standard Gaussian quadrature, and hence high accuracy can be achieved by a small number of Gaussian sample points. Since the spherical element subdivision method is performed in the physical coordinate system, it is a general algorithm for any kind of elements.

This paper is organized as follows. Detailed description of the spherical element subdivision method is presented in Section 2. Numerical examples are given in Section 3. The paper ends with conclusions in Section 4.

2. Spherical element subdivision method

In this section, the algorithm of the spherical element subdivision method is described in detail. Firstly, the source point is projected to the tangent plane of the element. Then two cases are

considered: the projection point is inside or outside the element. Fig. 1 shows the j-th step of the element subdivision. Fig. 1(a) and Fig. 1(b) are axonometric view and top view of the element subdivision, respectively. The meanings of the symbols in these figures are as follows:

P : the source point;
P' : the projection point of P;
V_i^j : the i-th vertex in the j-th step;
E_i^j : the i-th edge in the j-th step;
R_i^j : the line segment connecting P and V_i^j ;
EP_{ik}^j : the k-th intersection of E_i^j with the j-th sphere, k=1, 2;
RP_i^j : the projection point of intersection of R_i^j with the j-th sphere;
L_i^j : distance between P and V_i^j ;
D_i^j : distance between P and E_i^j ;
$L_{\min}$ = the shortest distance between the source point and the element to be subdivided;
$L_{\max} = \max\{L_i^j, D_i^j\}$.

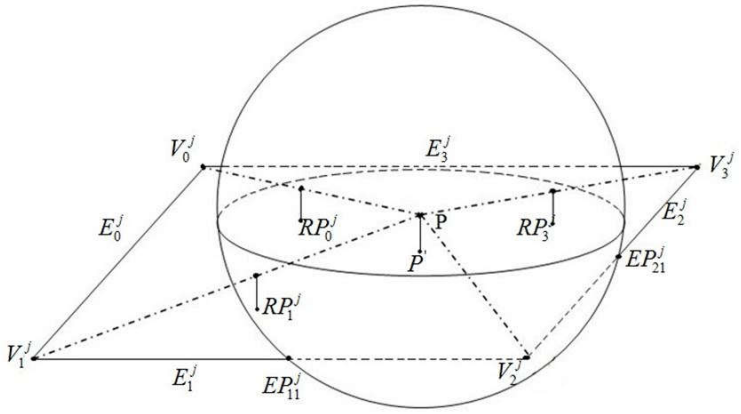

(a)

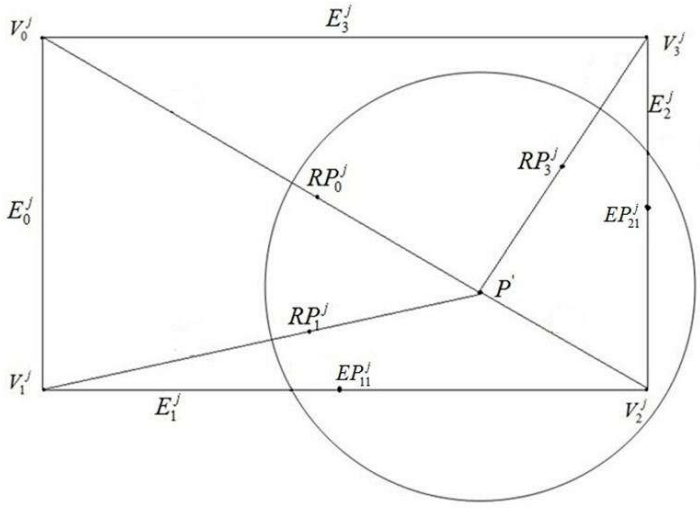

(b)

Figure 1. Element subdivision at the j-th step.
(a) Axonometric view of the element subdivision. (b) Top view of the element subdivision.

2.1 The case that the projection point P' is inside the element

In this case, the shortest distance between the source point and the element $L_{\min}$ equals the distance from P to P'. In each step, a sphere with its center at P is constructed, and its radius is defined as:

$$r_j = L_{\max} / 2^j \tag{1}$$

As the sphere is constructed, it interacts with the edges of the element and the line segment connecting P and V_i^j as shown in Fig. 1(a). Then the intersections are projected to the element and RP_i^j and EP_{ik}^j are obtained as shown in Fig. 1(b). These intersections are then connected in order. The element is subdivided into a certain number of patches as shown in Fig. 2. Polygon V_2^j - EP_{21}^j - RP_3^j - RP_0^j - RP_1^j - EP_{11}^j is obtained and will be subdivided in the next step. At the same time, the intersections V_2^j, EP_{21}^j, RP_3^j, RP_0^j, RP_1^j, EP_{11}^j take the place of the original vertexes to be the new vertexes for the next step. Edges will also be renewed. The algorithm is similar to the advancing front method which needs to update vertexes and edges in every step [29]. By repeating this process, a certain number of new patches will be obtained after each step. In the last step, the intersections and the projection of the source point will be connected as illustrated in Fig. 3(c). Fig. 3 shows the whole subdivision steps for a simple example.

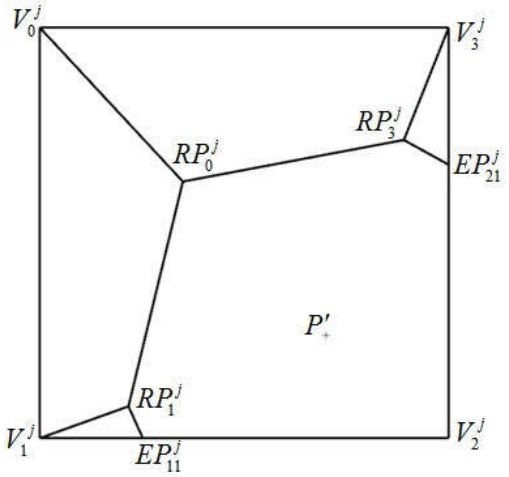

Figure 2. Connections and intersections at the j-th step.

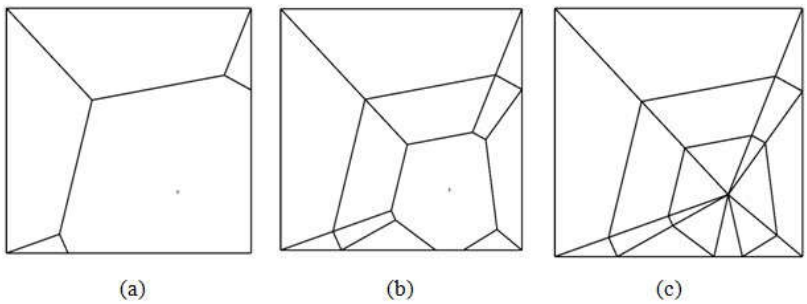

Figure 3. Subdivisions at various steps.

(a) The first step; (b) The second step; (c) The last step.

2.2 The case that the projection point P' is outside the element

In this case, P' is outside the element, $L_{\min}$ is computed by the following formula:

$$L_{min} = \sqrt{(L_1^2 + L_2^2)} \tag{2}$$

where L_1 is the distance between the source point P and its projection P'; L_2 is the shortest distance from P' to the element as shown in Fig. 4.

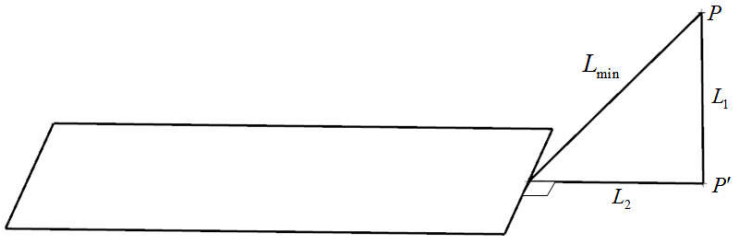

Figure 4. Nearest distance $L_{\min}$ in case that projection point is outside the element.

It can be seen from Fig. 5 that the intersections RP_3^j and RP_2^j are outside the element. If the intersections and vertexes are connected directly, the patches located outside the element will be obtained. To avoid this situation, RP_3^j and RP_2^j will be moved to EP_{21}^j and EP_{22}^j, respectively. Then the intersections and vertexes are connected using the former algorithm. After this operation, the patches are obtained as shown in Fig. 6.

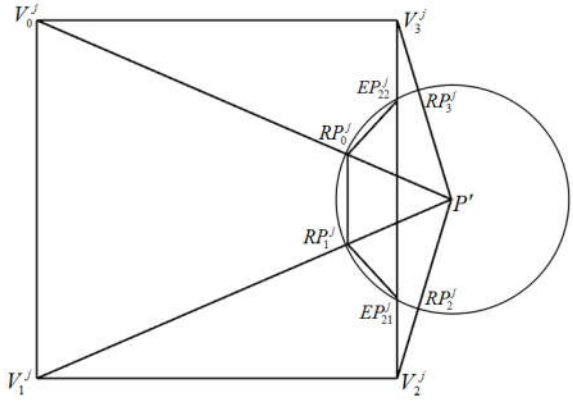

Figure 5. The case that the projection of the source point is outside the element.

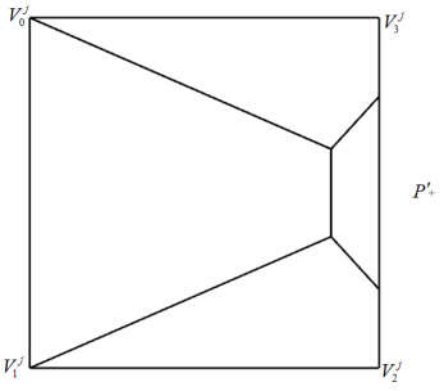

Figure 6. The patches obtained with the modified algorithm.

The main algorithm for creating patches is described by the following flow chart as shown in Fig. 7. When the radius of the *j*-th sphere $r_j < \eta_{\min} L_{\min}$, the element subdivision will be stopped.

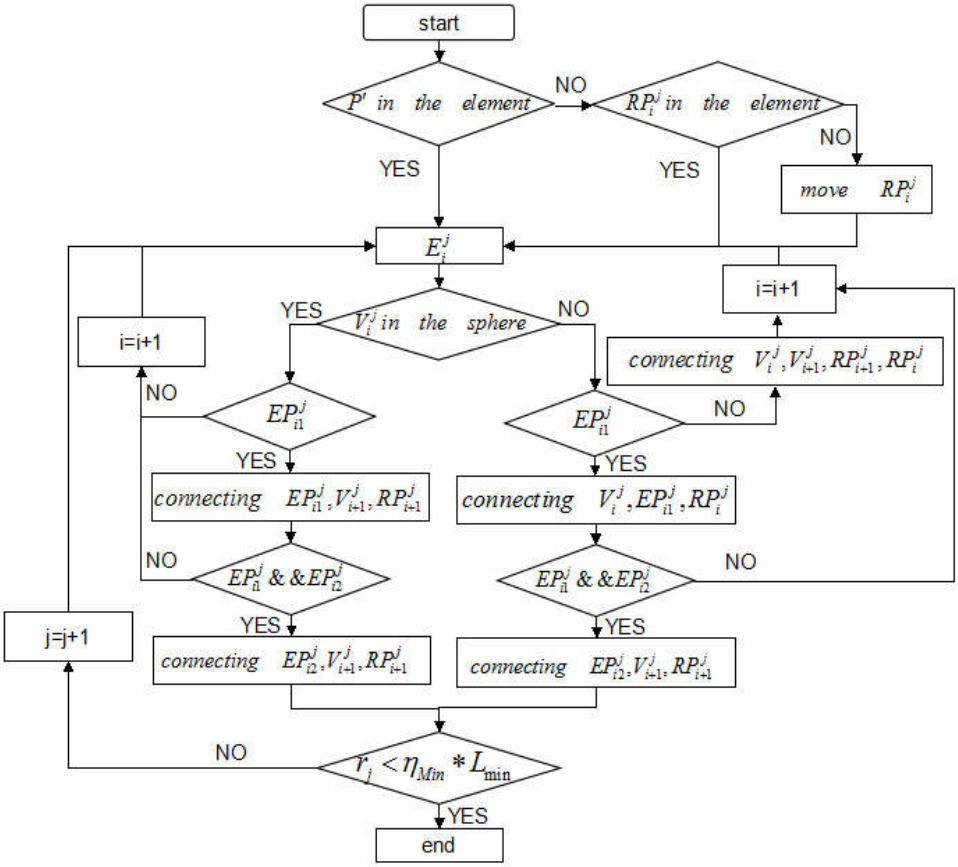

Figure 7. Flow chart of subdivision algorithm.

2.3 The optimization algorithm

From Fig. 3 it can be seen that total number of patches is very large, which will increase computational cost. At the same time, the shape of some patches is "bad", and it is unfavorable for accuracy and efficiency of the result. Thus the merging operation is proposed to deal with this situation.

"Bad" patch may occur in the following three cases. First, the distance between EP_{ik}^j and the vertex is smaller than an expected value d_1. Second, the distance between RP_i^j and the vertex is smaller than an expected value d_2. Third, the distance between RP_i^j and EP_{ik}^j is smaller than an expected value d_3. In any one of the three cases, one point will be merged into the other.

d_1、d_2、d_3 are defined as follows:

$$d_1 = edgeFactor * d(V_i^j, V_{i+1}^j)$$

$$d_2 = radFactor * r_j$$

$$d_3 = radFactor * r_j$$

where *edgeFactor*=0.1 and *radFactor*=0.1. After the merging operation, new patches are obtained as shown in Fig. 8. It can be seen that the number of patches is reduced and the shape of patches is improved obviously compared with that in Fig. 3.

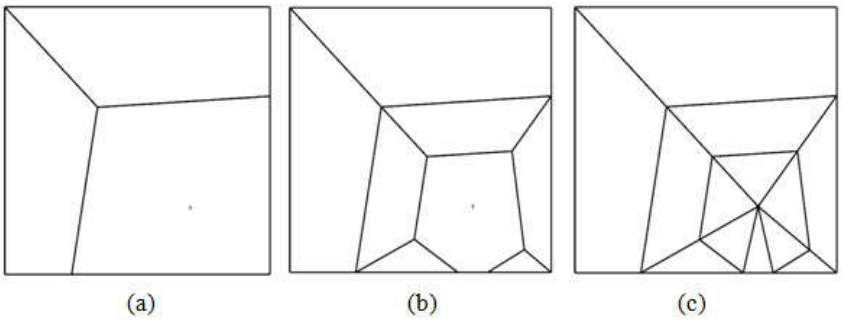

Figure 8. Element subdivision after merging operation.
(a) The first step; (b) The second step; (c) The last step.

With the detailed description above, it can be clearly seen that the shape of the patches obtained with our method is "good" due to the properties of sphere and the merging operation. Gaussian sample points are set denser around the projection point to get an accurate enough result. Away from the projection point, Gaussian sample points are sparsely distributed, which are much fewer but enough to grantee an accurate result, thus a large number of unnecessary Gaussian sample points are avoided. In the whole process, the number of patches and their size are determined adaptively by the location of source point. In a word, with the spherical element subdivision method, the nearly singular integrals can be solved with higher accuracy and less computational cost.

3. Numerical examples

To evaluate the effectiveness and accuracy of the proposed method, in this section, several comparisons are made between our method and other methods, such as distance transformation technique [19-21] and sinh transformation method [22-25]. For the purpose of error estimation, relative error is defined as follows:

$$\text{Relative Error}=\left|\frac{I_n - I_e}{I_e}\right| \tag{3}$$

where I_n and I_e are the numerical solution and exact solution of the integral, respectively.

The following integral is considered.

$$I=\int_\Gamma \frac{1}{4\pi r^p} N d\Gamma \tag{4}$$

where N is shape function, r stands for the distance between the source point and field point, and p represents the order of singularity (p = 1, 2 and 3).

In all numerical examples, the number of Gaussian sample points and the relative errors of different methods are listed. 'A' represents distance transformation technique. 'B' and 'C' are sinh

transformation method and sinh plus sigmoidal transformation method, respectively. The serendipity patch [30] is used in the proposed method. The patch obtained by our method becomes arc-shaped according to the location of the source point. The number of Gaussian points m is determined by [4, 31, 32]

$$m = \sqrt{\frac{2}{3}p + \frac{2}{5}}\left[-\ln(e/2)/10\right]\left[\left(\frac{8L}{3r_j}\right)^{\frac{3}{4}} + 1\right] \tag{5}$$

where e denotes the error tolerance. L is the length of the patch in integral direction. And r_j is the sphere radius defined in Eq. (1).

3.1 Example of planar element

In the first example, the numerical results by spherical element subdivision method and other methods for planar quadrilateral element are presented. The vertex coordinates of planar quadrilateral element are (0, 0, 0), (1, 0, 0), (1, 1, 0), (0, 1, 0) in the physical coordinate system. The source points are uniformly collocated along two lines as shown in Fig. 9 with $h_1 = 0.01$, $h_2 = 0.31$. The source points are numbered with Arabic numerals 0~8 (from top to bottom) and 9~18 (from left to right).

The patches obtained by our method for different locations of the source point are shown in Fig. 10 and Fig. 11. It can be seen that the patches are in "good" shape and size. The number of the Gaussian points and the relative errors of different methods are listed in Table 1.

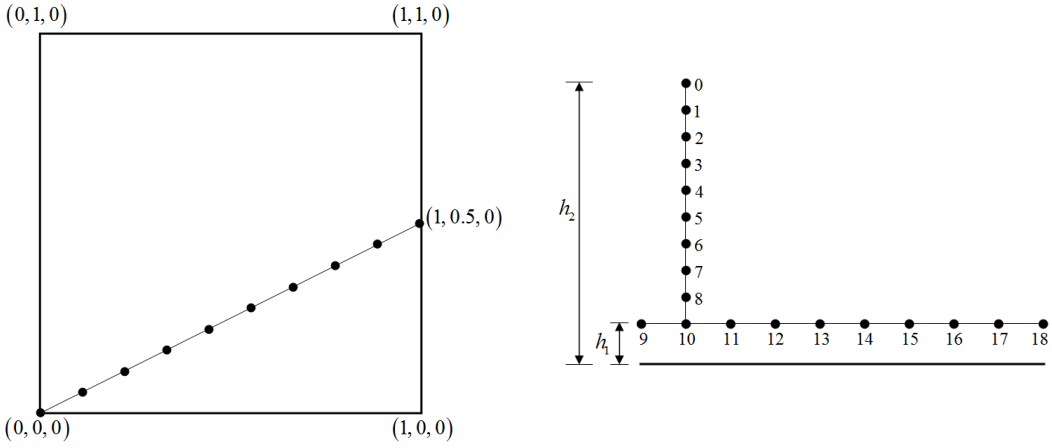

Figure 9. The planar element and the locations of the source point.

(a) Top view of the element and the source points. (b) Front view of the element and the source points.

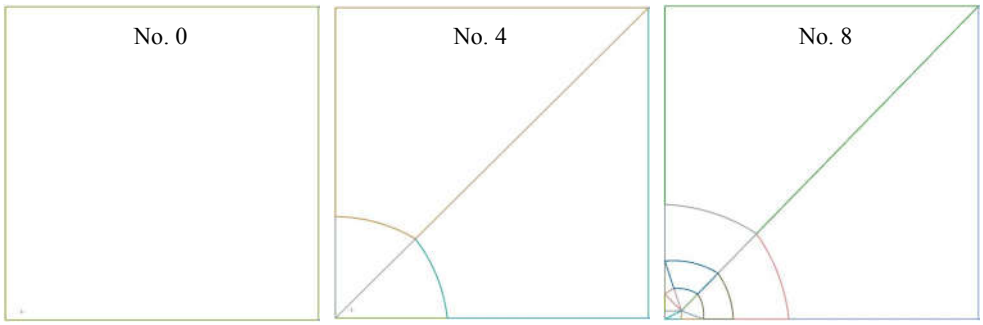

Figure 10. Subdivisions for locations of source point moving vertically.

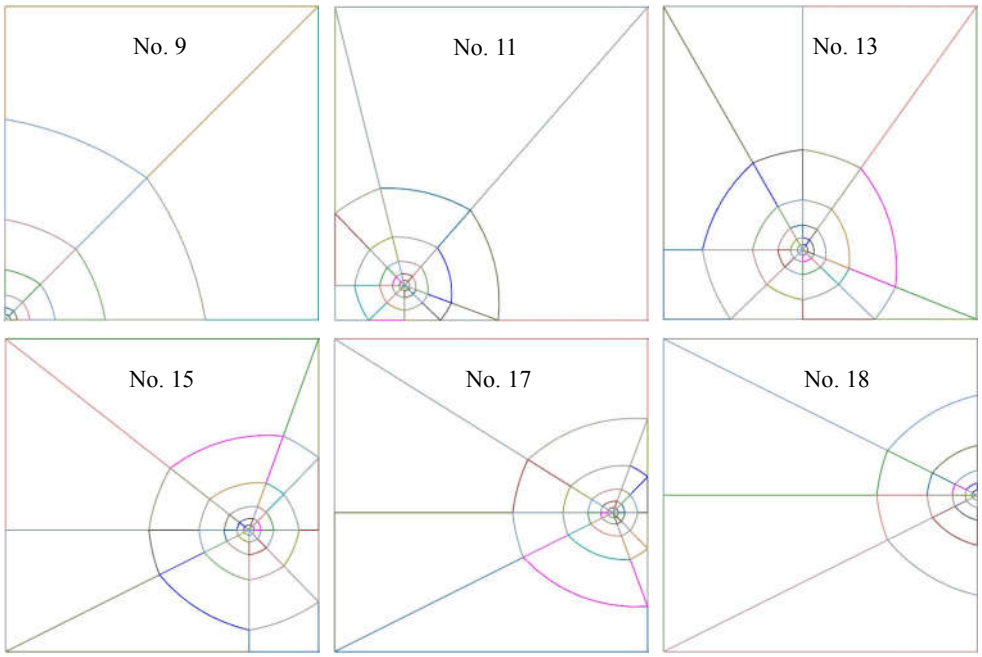

Figure 11. Subdivisions for locations of source point moving horizontally.

Table 1 Numerical results on a planar element.

Source point	Number of Gaussian points				Relative error			
	A	B	C	Our method	A	B	C	Our method
0	16	16	32	20	8.2532e-2	1.0558e-3	6.6394e-2	6.5731e-4
1	36	36	32	48	5.0534e-2	5.3359e-2	7.1744e-2	1.3996e-4
2	36	36	32	48	5.0012e-2	5.2459e-2	7.7893e-2	1.3638e-4
3	36	36	32	48	4.9347e-2	5.1067e-2	8.5146e-2	1.3607e-4
4	64	64	72	51	2.5306e-2	2.6415e-2	2.5382e-3	2.4964e-4
5	64	64	72	60	2.3976e-2	2.5566e-2	6.7412e-4	3.2417e-4
6	64	64	72	67	2.2432e-2	2.4541e-2	2.1559e-3	3.5848e-3
7	100	100	128	103	9.6748e-3	9.9299e-3	2.9758e-3	8.4397e-5
8	144	144	128	156	3.8426e-3	3.8947e-3	3.5677e-3	9.5223e-6
9	128	128	144	138	1.0865e-6	9.5217e-6	6.6043e-4	8.1271e-6
10	400	400	392	379	2.6568e-4	2.6585e-4	3.4633e-5	2.7282e-6
11	400	400	392	429	3.2202e-5	3.2284e-5	2.0068e-5	1.1443e-5
12	484	484	512	456	7.5196e-7	7.9038e-7	1.4281e-6	9.8228e-6
13	484	484	512	493	9.9456e-9	1.5887e-8	6.9512e-7	3.6412e-8
14	576	576	648	588	3.0531e-7	4.9294e-9	9.9510e-9	3.7380e-6
15	484	484	512	504	8.4589e-9	3.5748e-9	2.9291e-7	6.3274e-6
16	484	484	512	485	4.6799e-8	2.2363e-9	5.5429e-7	3.4578e-6
17	484	484	512	468	1.4887e-7	5.3185e-8	5.0080e-7	1.1082e-5
18	300	300	294	278	2.8474e-7	2.6004e-9	4.0155e-6	7.8094e-6

Table 1 shows that the accuracy obtained by the distance transformation method and sinh transformation method is higher than that by our method in some cases, but the accuracy obtained by our method is stable and acceptable for any locations of the source point.

3.2 Example of slender element

In this example, the spherical element subdivision method and other methods are performed on the slender element. The vertex coordinates of the slender element are (0, 0, 0), (10, 0, 0), (10, 1, 0), (0, 1, 0) in the physical coordinate system. The source points are uniformly collocated along two lines as shown in Fig. 12 with h_1 = 0.01, h_2 = 1.59. The source points are numbered with Arabic numerals 0~9 (from top to bottom) and 10~20 (from left to right).

The patches obtained by our method for different location of source points are shown in Fig. 13 and Fig. 14. It can be seen that the patches are in "good" shape and size. The number of the Gaussian points and the relative errors of different methods are listed in Table 2.

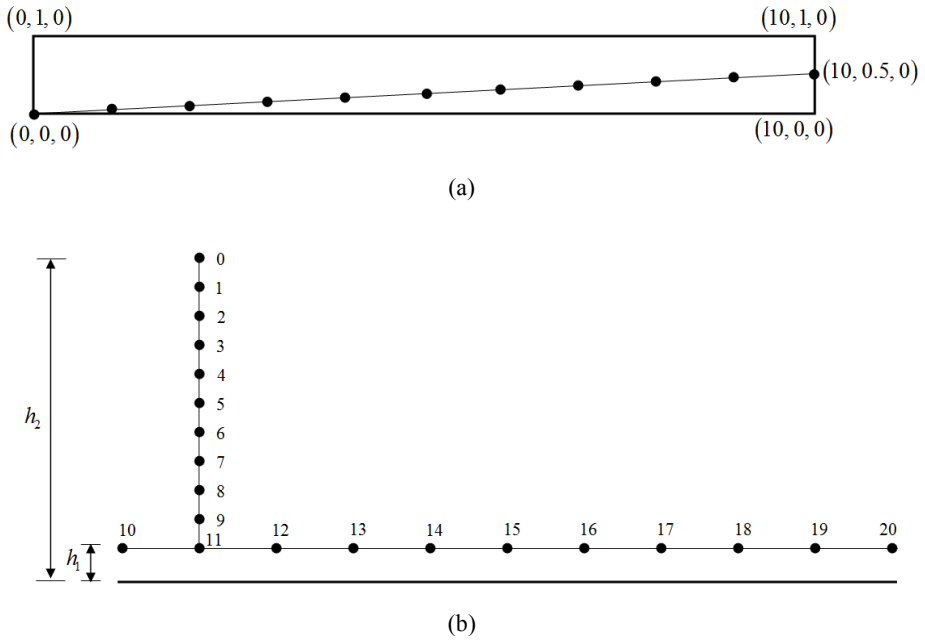

Figure 12. The slender element and the locations of the source point.
(a) Top view of the element and the source points. (b) Front view of the element and the source points.

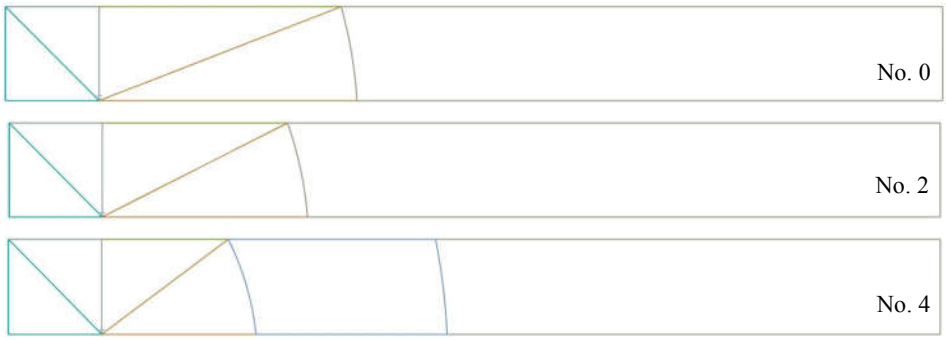

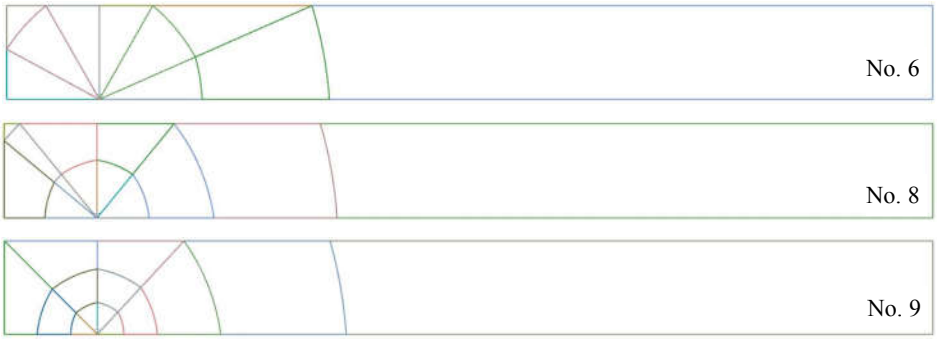

Figure 13. Subdivisions for locations of source point moving vertically.

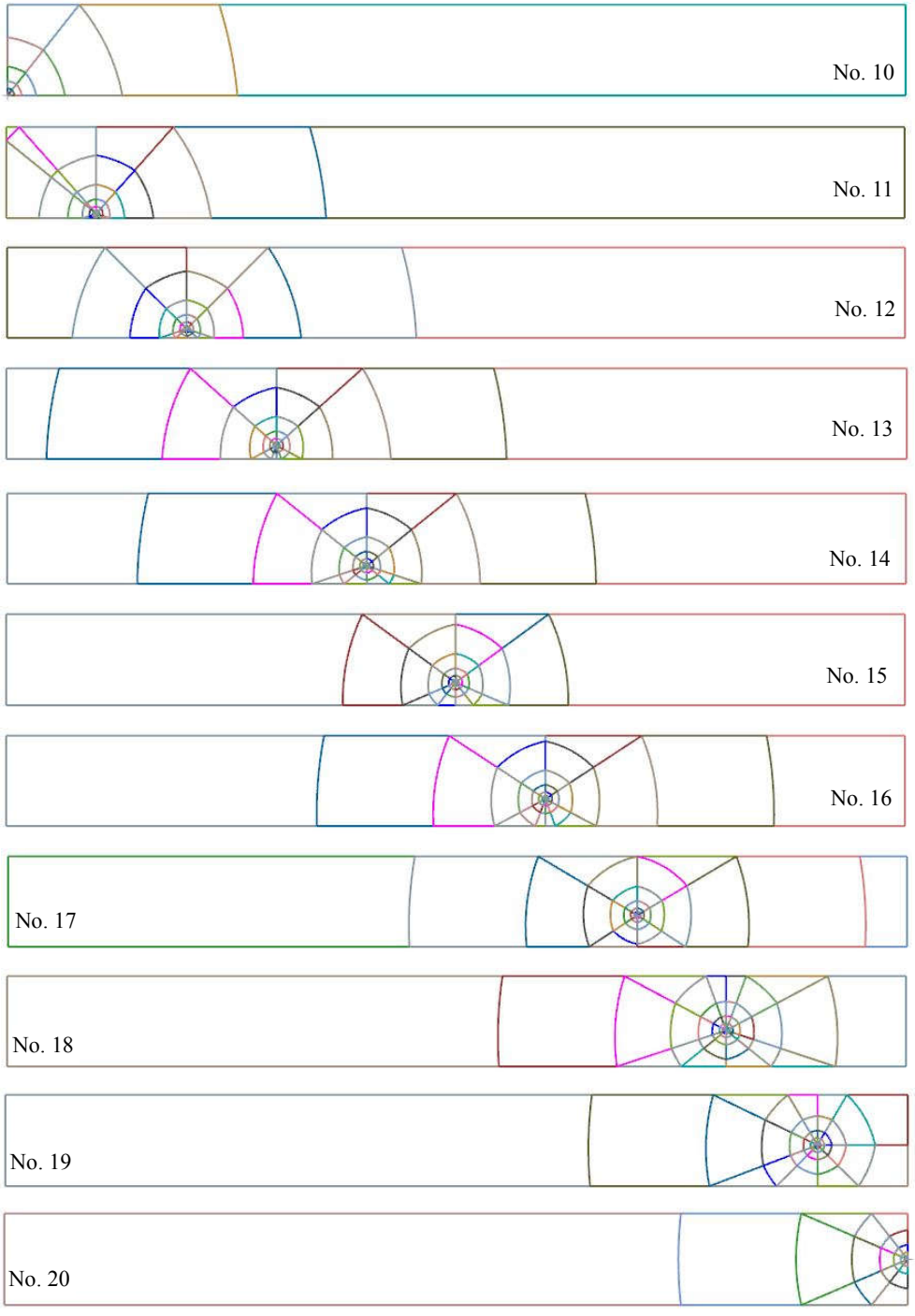

Figure 14. Subdivisions for locations of source point moving horizontally.

Table 2 Numerical results on a slender element.

Source point	Number of Gaussian points				Relative error			
	A	B	C	Our method	A	B	C	Our method
0	36	36	32	31	4.4066e-2	4.0780e-2	2.1717e-2	3.1182e-4
1	36	36	32	33	4.3592e-2	3.9798e-2	2.5394e-2	4.6344e-4
2	36	36	32	36	4.2985e-2	3.8641e-2	2.9745e-2	3.2901e-4
3	36	36	32	36	4.2167e-2	3.7270e-2	3.5082e-2	5.2164e-4
4	36	36	32	45	4.1021e-2	3.5622e-2	4.1879e-2	2.0326e-5
5	64	64	32	49	1.5313e-2	1.5096e-2	5.0868e-2	1.4442e-5
6	64	64	72	66	1.6111e-2	1.5679e-2	9.5684e-3	2.6152e-3
7	100	100	72	96	2.9382e-3	3.0566e-3	8.5817e-3	6.3826e-5
8	144	144	128	129	2.2749e-3	2.1928e-3	4.8821e-3	4.7677e-5
9	144	144	128	154	2.9570e-3	2.8866e-3	7.8248e-3	3.4229e-5
10	162	162	196	175	8.0740e-6	6.2623e-7	4.6241e-5	6.6550e-6
11	484	484	512	506	5.1797e-3	5.1809e-3	1.1366e-2	3.4709e-6
12	484	484	512	511	1.0518e-2	1.0519e-2	1.4348e-2	9.6752e-6
13	484	484	512	522	1.1748e-2	1.1750e-2	7.2528e-3	8.9188e-6
14	576	576	648	586	9.4047e-4	9.4064e-4	9.0105e-3	4.2710e-6
15	576	576	648	584	1.6694e-2	1.6694e-2	3.6332e-2	1.3552e-6
16	576	576	648	586	8.8486e-3	8.8484e-3	2.6178e-3	6.5219e-6
17	576	576	512	542	6.5545e-3	6.5547e-3	2.7797e-2	6.7369e-6
18	676	676	648	628	7.6170e-4	7.6179e-4	7.0510e-4	6.9944e-6
19	576	576	648	584	3.2067e-4	3.2078e-4	7.1817e-4	7.9095e-6
20	363	363	294	336	1.9924e-6	1.9767e-6	2.0768e-6	9.0218e-7

From Table 2, it can be seen that with equivalent number of Gaussian points, our method achieves much better the accuracy than that other methods. Again, the accuracy obtained by our method for all locations of the source point is stable. Therefore, our method is more suitable for evaluating nearly singular integrals on slender elements.

4. Conclusions

A general element spherical subdivision method has been presented in this paper for evaluating nearly singular integrals in 3D BEM. With the proposed method, the element is subdivided by a sequence of spheres centered at the source point, and the obtained patches are automatically refined as they approach the projection of the source point. Therefore, each patch is ensured to be “good” in shape and size, no matter where the source point locates. In addition, the spherical element subdivision method is performed in the physical coordinate system, thus it is a general algorithm for any kind of boundary element. Through the numerical examples, it can be seen that the accuracy obtained by our method is stable and acceptable for any locations of the source point. With equivalent number of Gaussian points, our method achieves much better the accuracy than that other methods on slender element. We can conclude that the proposed method is more suitable for evaluating nearly singular integrals. Extension of our method for high order elements is ongoing.

References

[1] Brebbia CA, Telles JCF, and Wrobel LC. Boundary element techniques: theory and applications in engineering. Vol. 5. Berlin: Springer-Verlag; 1984.

[2] Han PS. A Galerkin boundary element formulation with moving singularities. *Engineering Computations* 1984; 1; 232-236.

[3] Provatidis C. A boundary element method for axisymmetric potential problems with non-axisymmetric boundary conditions using fast fourier transform. *Engineering Computations* 1998; 15; 428-449.

[4] Gao XW, Davies TG. Adaptive integration in elasto-plastic boundary element analysis. *Journal of the Chinese Institute of Engineers* 2000; 23; 349-356.

[5] Zhang JM, Qin XY, Han X, Li GY. A boundary face method for potential problems in three dimensions. *International Journal for Numerical Methods in Engineering* 2009; 80; 320-337.

[6] Chen CH, Chen CS, Pan E, Tseng HC, Yu PS. Boundary element analysis of mixed-mode stress intensity factors in an anisotropic cuboid with an inclined surface crack. *Engineering Computations* 2009; 26; 1056-1073.

[7] Liu YJ. Analysis of shell-like structures by the boundary element method based on 3-D elasticity: formulation and verification. *International Journal for Numerical Methods in Engineering* 1998; 41; 541-558.

[8] Liu YJ, Fan H. Analysis of the thin piezoelectric solids by the boundary element method. *Computer Methods in Applied Mechanics and Engineering* 2002; 191; 2297–2315.

[9] Zhang YM, Gu Y, Chen JT. Boundary element analysis of 2D thin walled structures with high-order geometry elements using transformation. *Engineering Analysis with Boundary Elements* 2011; 35; 581-586.

[10] Aliabadi MH, Martin D. Boundary element hyper-singular formulation for elastoplastic contact problems. *International Journal for Numerical Methods in Engineering* 2000; 48; 995-1014.

[11] Zhang D, Rizzo FJ, Rudolphi TJ. Stress intensity sensitivities via hypersingular boundary integral equations. *Computational Mechanics* 1999; 23; 389-396.

[12] Dirgantara T, Aliabadi MH. Crack growth analysis of plates loaded by bending and tension using dual boundary element method. *International Journal of Fracture* 2000; 105; 27-47.

[13] Niu ZR, Wendland WL, Wang XX, Zhou HL. A semi-analytic algorithm for the evaluation of the nearly singular integrals in three-dimensional boundary element methods. *Computer Methods in Applied Mechanics and Engineering* 2005; 31; 949–964.

[14] Zhou HL, Niu ZR, Cheng CZ, Guan ZW. Analytical integral algorithm applied to boundary layer effect and thin body effect in BEM for anisotropic potential problems. *Computers & structures* 2008; 86; 1656–1671.

[15] Xie GZ, Zhang JM, Qin XY, Li GY. New variable transformations for evaluating nearly singular integrals in 2D boundary element method. *Engineering Analysis with Boundary Elements* 2011; 35: 811-817.

[16] Xie GZ, Zhang JM, Huang C, Lu CJ, Li GY. Calculation of Nearly Singular Boundary Element Integrals in Thin Structures Using an Improved Exponential Transformation. *Computer Modeling in Engineering & Sciences* 2013; 94(2): 139-157.

[17] Xie GZ, Zhou FL, Zhang JM, Zheng XS, Huang C. New variable transformations for evaluating nearly singular integrals in 3D boundary element method. *Engineering Analysis with Boundary Elements* 2013; 37: 1169-1178.

[18] Xie GZ, Zhang JM, Dong YQ, Huang C, Li GY. An improved exponential transformation for nearly singular boundary element integrals in elasticity problems. *International Journal of Solids and Structures* 2014; 51: 1322-1329.

[19] Ma H, Kamiya N. Distance transformation for the numerical evaluation of near singular boundary integrals with various kernels in boundary element method. *Engineering Analysis with Boundary Elements* 2002; 26; 329–339.

[20] Ma H, Kamiya N. A general algorithm for the numerical evaluation of nearly singular boundary integrals of various orders for two- and three-dimensional elasticity. *Computational mechanics* 2002; 29; 277–288.

[21] Qin XY, Zhang JM, Xie GZ, Zhou FL, Li GY. A general algorithm for the numerical evaluation of nearly singular integrals on 3D boundary element. *Journal of Computational and Applied Mathematics* 2011; 235; 4174-4186.

[22] Johnston BM, Johnston PR, Elliott D. A sinh transformation for evaluating two-dimensional nearly singular boundary element integrals. *International journal for numerical methods in engineering* 2007; 69(7); 1460-1479.

[23] Johnston PR, Elliott D. A sinh transformation for evaluating nearly singular boundary element integrals. *International journal for numerical methods in engineering* 2005; 62(4); 564-578.

[24] Johnston BM, Johnston PR, Elliott D. A new method for the numerical evaluation of nearly singular integrals on triangular elements in the 3D boundary element method. *Journal of Computational and Applied Mathematics* 2013; 245; 148-161.

[25] Gu Y, Chen W, Zhang C. The sinh transformation for evaluating nearly singular boundary element integrals over high-order geometry elements. *Engineering Analysis with Boundary Elements* 2013; 37(2); 301-308.

[26] Gao XW. An effective method for numerical evaluation of general 2D and 3D high order singular boundary integrals. Computer Methods in Applied Mechanics & Engineering 2010; 199; 2856-2864.

[27] Gao XW, Zhang JB, Zheng BJ, Zhang C. Element-subdivision method for evaluation of singular integrals over narrow strip boundary elements of super thin and slender structures. Engineering Analysis with Boundary Elements 2016; 66; 145-154.

[28] Tanaka M, Zhang JM, Matsumoto T. Boundary-type meshless solution of potential problems: comparison between singular and regular formulations in hybrid BNM. *Transactions of JASCOME. Journal of Boundary Element Methods* 2003; 20; 21-26.

[29] Wu B, Wang S. Automatic triangulation over three-dimensional parametric surfaces based on advancing front method. *Finite Elements in Analysis and Design* 2005; 41(9); 892-910.

[30] Zhong YD, Zhang JM, Dong YQ, Li Y, Lin WC and Tang JY. A serendipity triangular patch for evaluating weakly singular boundary integrals. Engineering Analysis with Boundary Elements 2016; 69; 86-92.

[31] Bu S, Davies TG. Effective evaluation of non-singular integrals in 3D BEM. *Advances in Engineering Software* 1995; 23(2); 121-128.

[32] Lachat JC, Watson JO. Effective numerical treatment of boundary integral equations: A formulation for three-dimensional elastostatics. *International Journal for Numerical Methods in Engineering* 1976; 10(5); 991-1005.